Scientific Research Publishing

Journal of Modern Physics, 2023, 14, 722-740
https://www.scirp.org/journal/jmp
ISSN Online: 2153-120X
ISSN Print: 2153-1196

Propagation Characteristics of Ultrasonic Guided Waves in Grouted Rockbolt Systems with Bond Defects under Different Confining Conditions

Shuisheng Yu[1*], Jin Chen[2], Yawei Wang[1], Honghao Yang[1], Shucan Lu[1]

[1]School of Architectural Engineering, Zhongyuan University of Technology, Zhengzhou, China
[2]School of Economics and Management, Zhongyuan University of Technology, Zhengzhou, China
Email: *yuss.1987@163.com

How to cite this paper: Yu, S.S., Chen, J., Wang, Y.W., Yang, H.H. and Lu, S.C. (2023) Propagation Characteristics of Ultrasonic Guided Waves in Grouted Rockbolt Systems with Bond Defects under Different Confining Conditions. *Journal of Modern Physics*, **14**, 722-740.
https://doi.org/10.4236/jmp.2023.145041

Received: March 16, 2023
Accepted: April 23, 2023
Published: April 26, 2023

Abstract

A rockbolt acting in the rock mass is subjected to the combined action of the pull-out load and confining pressure, and the bond quality of the rockbolt directly affects the stability of the roadway and cavern. Therefore, in this study, confining pressure and pull-out load are applied to grouted rockbolt systems with bond defects by a numerical simulation method, and the rockbolt is detected by ultrasonic guided waves to study the propagation law of ultrasonic guided waves in defective rockbolt systems and the bond quality of rockbolts under the combined action of pull-out load and confining pressure. The numerical simulation results show that the length and location of bond defects can be detected by ultrasonic guided waves under the combined action of pull-out load and confining pressure. Under no pull-out load, with increasing confining pressure, the low-frequency part of the guided wave frequency in the rockbolt increases, the high-frequency part decreases, the weakening effect of the confining pressure on the guided wave propagation law increases, and the bond quality of the rockbolt increases. The existence of defects cannot change the strengthening effect of the confining pressure on the guided wave propagation law under the same pull-out load or the weakening effect of the pull-out load on the guided wave propagation law under the same confining pressure.

Keywords

Grouted Rockbolt Systems, Bond Defect, Pull-Out Load, Confining Pressure, Ultrasonic Guided Wave

1. Introduction

The occurrence environment of a deep rock mass is complex when it is in a state of "three highs and one disturbance" (high ground stress, high seepage pressure, high earth temperature and mining disturbance) [1]. A rockbolt acting in the rock mass is always subjected to the combined action of the pull-out load and confining pressure. The construction quality of the rockbolt (such as the quality of the rockbolt bond, whether the length of the rockbolt is consistent with the design length, whether the mortar is full, that is, whether the rockbolt has played the expected role, etc.) directly affects the stability of the roadway, chamber and slope. The construction of rockbolts is a concealed project, with the rockbolt and grouted agent being hidden [2] [3], the length of the rockbolt being insufficient [4] [5] or whether it contains natural joints [6] [7] [8]. The bond quality of the rockbolt and its defects are closely related to the stability and safety of the surrounding rock and roadway slope, so it is necessary to detect the bond defects and quality of the rockbolt under the combined action of pull-out load and confining pressure.

In the detection of bond defects and quality, Xu *et al.* [3] determined the location of bond defects by means of experiments and numerical simulations from a mechanical point of view. Lin *et al.* [4] used the impact echo method to detect the bond length, and their results showed that the method could detect the bond length well when it was clear whether the rockbolt was grouted or not. The attenuation and group velocity of ultrasonic guided waves in rockbolts were studied by Cui *et al.* [9], and the influence of insufficient rockbolts and mortar on grouted rockbolts was confirmed and verified by experiments. Zhang *et al.* [10] used the Hilbert-Huang signal processing method to analyse the detection signals of various complete bond and defective bond models. This method could clearly identify the defects and the reflected signals at the bottom of the rockbolt to more accurately deduce the defect position and bond length. Zhang *et al.* [11] used self-designed nondestructive testing experimental systems for bond quality to detect whether bond systems have defects and determined the number of defects by using the multiscale entropy method. Wang *et al.* [12] used ultrasonic guided wave technology to detect the initial corrosion of reinforced concrete with defects. Their results showed that the method could identify debonding and crack propagation at the interface between the steel bar and concrete. Liu *et al.* [13] used the finite element method to simulate the propagation process of ultrasonic guided waves in defective rockbolts, used the improved adaptive noise complete ensemble empirical mode decomposition (ICEEMDAN) method to process the reflected signals of ultrasonic guided waves, and obtained the arrival time of the reflected wave of defects according to the peak value of the decomposed natural mode function, thus determining the location and length of bond defects. Liu *et al.* [14] analysed the influence of tensile stress on the propagation characteristics of ultrasonic guided waves in steel cables based on a fast Fourier transform, and their results showed that the energy transfer of ultrasonic guided waves increased with increasing tensile force. Yu *et al.* [15] used a rockbolt pull-out and stress

wave detection test device to pull out the rockbolt and detect its bond quality under different loads and then used the wavelet transform to carry out wavelet multiscale and frequency spectrum analysis on the detection signal, determined the debonding length of the rockbolt under the pull-out load and evaluated the bond quality of the rockbolt. Ivanovic and Neilson [16] used a magnetostrictive nondestructive testing method to evaluate the effective length of a rockbolt under a pull-out load without considering the defects in the grouted rockbolt system. Yu *et al.* [17] used ultrasonic guided waves to detect bond defects under different pull-out loads to determine bond quality but did not consider confining pressure. Yu *et al.* [18] used ultrasonic guided waves to detect rockbolts under different pull-out loads and confining pressures and studied the bond quality of rockbolts but did not consider the influence of bond defects.

Based on the above research, it can be seen that there is relatively little research on the detection and propagation law of bond quality by using ultrasonic guided waves, especially under the combined action of pull-out load and confining pressure. However, the stress change in the rock mass is one of the important factors affecting the bond strength of the rockbolt and the propagation of stress waves in the rockbolt. Therefore, a numerical simulation method was used to realize the influence of stress in rockbolt support by applying confining pressure in this study. Fully grouted rockbolt systems with bond defects under the combined action of pull-out load and confining pressure were detected to determine the location of bond defects and the influence of pull-out load and confining pressure on the propagation law of ultrasonic guided waves and to evaluate the bond quality of rockbolts.

2. The Establishment of the Numerical Model and Experimental Verification

Defects often appear in grouted rockbolt systems, and the existence of defects always affects structural safety. Therefore, the bond quality of grouted rockbolt systems with defects is studied under pull-out load and confining pressure.

In the numerical simulation, the size of the sample refers to the sample size of the laboratory test in reference [19]. A hollow cylinder concrete sample was used to simulate the surrounding rock, with an outer diameter of 150 mm, an inner diameter of 40 mm and a length of 1500 mm. hollow cylinder cement mortar was used to simulate the grouted agent, with an outer diameter of 40 mm and an inner diameter of 25 mm. The rockbolt diameter was 25 mm, the length was 2500 mm, the B-end of the grouted rockbolt was 700 mm away from the A-end, the defect-end was 700 mm away from the B-end of the grouted rockbolt system, and the defect length was 100 mm. The dimension parameters of the grouted rockbolt system are shown in **Figure 1**.

2.1. Modelling of the Concrete, Cement Mortar, and Rockbolt

The concrete damage plasticity model (CDPM) used herein to simulate the

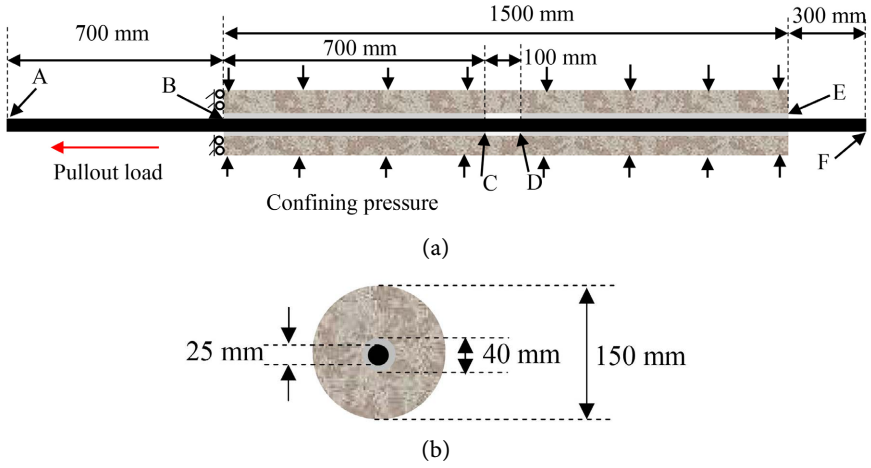

Figure 1. Grouted rockbolt systems model with one bond defect. (a) Size of grouted rockbolt systems; (b) Diameter of grouted rockbolt systems.

mechanical behaviour of quasibrittle materials (*i.e.*, the concrete and cement mortar) was proposed for ABAQUS by Lee and Fenves (1998) [20]. The CDPM considers isotropic damaged elasticity in combination with isotropic tensile and compressive plasticity to represent the inelastic behaviour of concrete [21]. The model exhibits multiple advantages, including its simplicity and numerical stability.

We introduced a damage variable into the CDPM and used the damage plasticity to determine the uniaxial tension and compression constitutive relationships of our concrete (cement mortar) specimens. The concrete (cement mortar) elastic modulus was reduced to simulate the degradation of the concrete unloading stiffness under elevated levels of strain. The CDPM assumes that concrete (cement mortar) failure results from tensile cracking and crushing.

Based on test results in the reference [15], the rockbolt experiences elastic ascent, yielding, hardening and complete slip without breaking. Therefore, the rockbolt is set as an elastoplastic material in ABAQUS. The material parameters of the rockbolt, concrete and cement mortar are presented in **Table 1**.

2.2. Modelling of Bond Behaviour

The interface bond behaviour can be modelled by cohesive elements [22] [23] [24] or surface-based cohesive behaviour [19] [25] [26] using the traction-separation law in Abaqus. The interface thickness of our specimen is negligibly small, and we sought to reduce the calculation time, so we modelled the interface bond behaviour between the rockbolt (concrete) and cement mortar by the surface-based cohesive behaviour in this study.

The damage laws for the cohesive behaviour in shear directions (see **Figure 2**) are defined according to the following steps: 1) linear elastic shear stress-slip relations by defining the elastic bond stiffness; 2) damage initiation criteria, which can be defined by the maximum bond shear stress; and 3) damage evolution laws for the exponential softening branch of the bond [27].

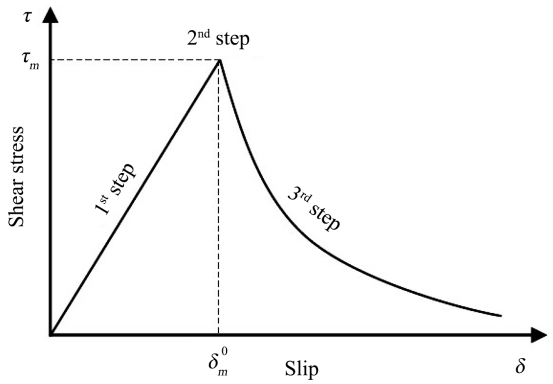

Figure 2. Damage law for the cohesive behavior [27].

Table 1. Material properties of the rockbolt, concrete and cement mortar [15].

Ingredient	Density (kg/m³)	Elastic modulus (GPa)	Poisson's ratio
Rockbolt	7850	210	0.3
Cement mortar	2100	20	0.19
Concrete	2300	33	0.23

The uncoupled constitutive relation of the traction-separation behaviour as expressed in Abaqus is as follows:

$$T = \begin{Bmatrix} t_n \\ t_s \\ t_t \end{Bmatrix} = \begin{bmatrix} k_{nn} & 0 & 0 \\ 0 & k_{ss} & 0 \\ 0 & 0 & k_{tt} \end{bmatrix} \begin{Bmatrix} \delta_n \\ \delta_s \\ \delta_t \end{Bmatrix} = K\delta \tag{1}$$

where t_n is the nominal stress in the normal direction; t_s and t_t are the nominal stresses in two local shear directions; k_{nn}, k_{ss} and k_{tt} are the corresponding stiffness coefficients; and δ_n, δ_s and δ_t are the corresponding displacements.

k_{nn}, k_{ss} and k_{tt} are given by [22]:

$$k_{ss} = k_{tt} = \tau_m / \delta_m^0 \tag{2}$$

$$k_{nn} = 100k_{ss} = 100k_{tt} \tag{3}$$

where τ_m is the maximum shear strength and δ_m^0 is the slip value at the maximum shear strength, namely, the effective displacement at the initiation of the damage.

The stress components of the traction-separation model are affected by the damage.

$$t_n = (1-d)\overline{t}_n \tag{4}$$

$$t_s = (1-d)\overline{t}_s \tag{5}$$

$$t_t = (1-d)\overline{t}_t \tag{6}$$

where $\overline{t}_n$, $\overline{t}_s$ and $\overline{t}_t$ are the stress components predicted by the elastic traction-separation behaviour for the current strains without damage. d is the dam-

age variable. For exponential softening,

$$d = 1 - \left\{ \frac{\delta_m^0}{\delta_m^{\max}} \right\} \left\{ 1 - \frac{1 - \exp\left(-\alpha \left(\frac{\delta_m^{\max} - \delta_m^0}{\delta_m^f - \delta_m^0} \right) \right)}{1 - \exp(-\alpha)} \right\} \tag{7}$$

where δ_m^f is the effective displacement at complete failure. $\delta_m^{\max}$ is the maximum value of the effective displacement attained during the loading history. α is a nondimensional material parameter that defines the rate of damage evolution.

In the numerical model, the grouted rockbolt systems are simulated by four-node bilinear axisymmetric quadrilateral elements with reduced integration (CAX4R). The interface at the loaded end of the concrete is fixed during the test for the boundary condition in the grouted rockbolt systems. On the basis of extensive trials, a mesh size of 2 mm for the rockbolt and cement mortar and a mesh size of 5 mm for the concrete are deemed adequate to obtain sufficiently accurate results. The stiffness matrix is singular when the damage value, scalar stiffness degradation (SDEG), is equal to 1. Therefore, the maximum damage value was limited to 0.9998 to avoid the occurrence of a singular stiffness matrix [27].

2.3. Numerical Test Procedure

Conventional rockbolts acting in deep rock masses have a stress variation of 10 - 15 MPa during service [28]. Therefore, in the numerical simulations, the confining pressures are 0, 5, 10 and 15 MPa, which are used to study the effect of confining pressure on the propagation law of ultrasonic guided waves and to determine the bond quality of rockbolts under confining pressure.

The testing procedure was as follows. First, the grouted rockbolt was maintained without pull-out force and confining pressure, the ultrasonic guided wave was excited at the A-end. Next, the 5 MPa, 10 MPa and 15 MPa confining pressure was applied, respectively, the rockbolt was detected by ultrasonic wave in absence of pull-out load. Rockbolts with bond defects are often subjected to the combined effect of axial and radial loads during service. Therefore, the propagation law of guided waves in grouted rockbolt systems is explored considering the combined effect of confining pressure and pull-out load in two cases: 1) the same pull-out load with different confining pressures and 2) the same confining pressure with different pull-out loads. When the pull-out load keep unchanged, the confining pressure was increased to 5 MPa, 10 MPa and 15 MPa, and the above steps were repeated. When the confining pressure keep unchanged, the pull-out load was increased to 25 kN, 50 kN, 75 kN and 100 kN, the ultrasonic guided wave was tested according to the above steps. According to the results of ultrasonic guided wave testing, the bond quality of rockbolt under the combined action of pull-out load and confining pressure were analyzed.

2.4. Experimental Verification

The ultrasonic guided wave is used for detection in the numerical simulation, and the cut-off frequency of the guided wave in the grouted rockbolt free of loading is 22 kHz. Therefore, the input waveform of the ultrasonic guided wave was the sine wave with 10 cycles and 22 kHz frequency obtained by the Hanning window (**Figure 3**) [15]. The ultrasonic guided wave was excited at the A-end, and the wave was received at the F-end. The comparison between the numerical and experimental results is shown in **Figure 4** [15]. The signal received at the other end was in good agreement with the experimental result, which indicated that the numerical model could simulate the guided wave propagation in grouted rockbolt systems.

3. Propagation of Ultrasonic Guided Wave in Grouted Rockbolt Systems with Bond Defects

3.1. Influence of Confining Pressure on Guided Wave Propagation in Absence of Pull-Out Load

The ultrasonic guided wave signal was excited at the A-end (**Figure 1**). **Figure 5** displays the propagation of ultrasonic guided waves in grouted rockbolt systems

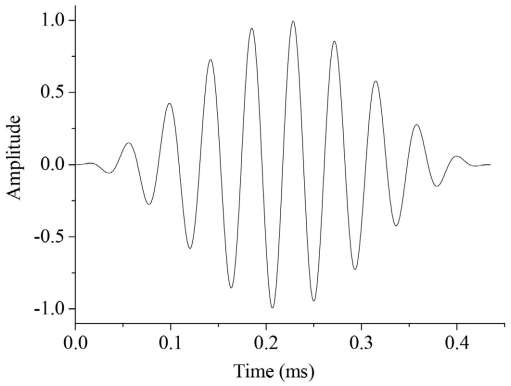

Figure 3. Excitation signal input for the numerical simulation [15].

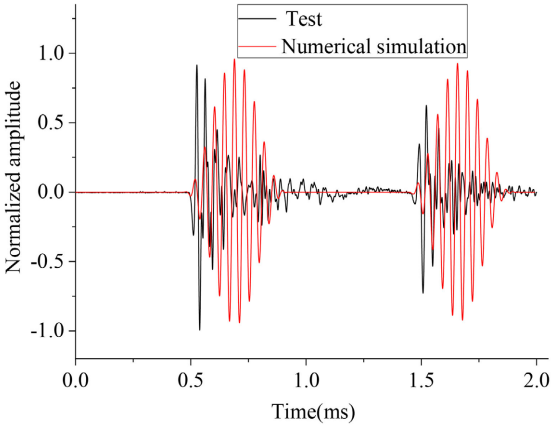

Figure 4. Comparison of numerical and test results of wave propagation in free rockbolt [15].

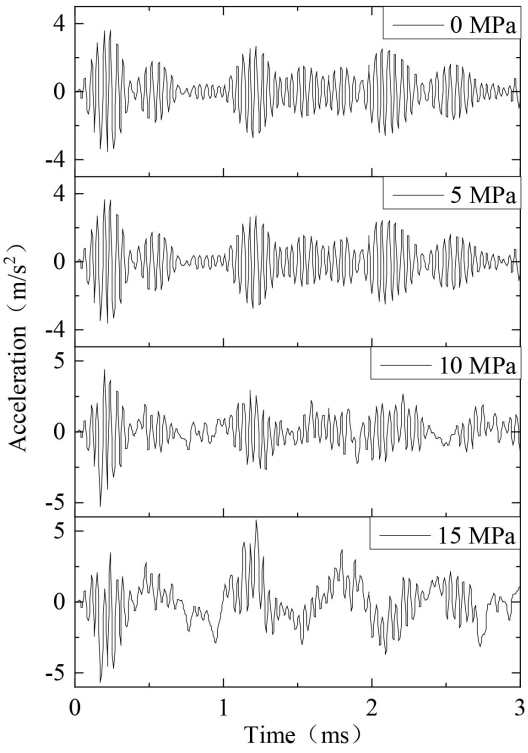

Figure 5. The influence of confining pressure on guided wave propagation in absence of pull-out load.

with bond defects in the absence of a pull-out load. The law of guided wave propagation gradually deteriorates with increasing confining pressure, and this phenomenon is the same as the propagation law of guided waves in grouted rockbolt systems without bond defects [18], while the echo wave packet at the bond defects fluctuates with increasing confining pressure, and the presence of bond defects cannot change the weakening effect of the confining pressure on the propagation law of guided waves.

The variation of frequency in the guided wave with the confining pressure in absence of pull-out load is shown in **Figure 6**. In the grouted rockbolt systems with bond defect, the low frequency part of the guided wave frequency in the rockbolt increases and the high frequency part decreases with the increase of the confining pressure. In **Figure 7**, the ratio Q of the maximum amplitude of guided wave at low frequency to that at high frequency increases exponentially with the increase of the confining pressure, indicating that the presence of bond defects cannot change the trend of the Q value with the confining pressure.

The propagation process of guided waves in grouted rockbolt systems with bond defects under different confining pressures without a pull-out load is shown in **Figure 8**. The wave propagation is relatively good without confining pressure, and the wave propagation arrives at the B-end of the rockbolt at 0.3 ms and then continues to spread along the rockbolt and reach the bond defect. In the bond defect, part of the guided wave continues to spread, and the other part is reflected back to the loading end; the peak echo energy arrives at the loading end at 1.2

ms. Under a 5 MPa confining pressure, the wave propagation is slightly less regular due to the effect of the confining pressure, but at 0.7 ms, the peak wave energy can be clearly seen when arriving at the bond defect from the propagation cloud map, and then part of the guided wave is reflected back to the loading end, and part continues to propagate to the distal end of the grouted rockbolt systems. As the confining pressure increases to 10 MPa and 15 MPa, the law of guided wave propagation becomes increasingly worse, which further indicates that the confining pressure has a weakening effect on guided wave propagation without a pull-out load.

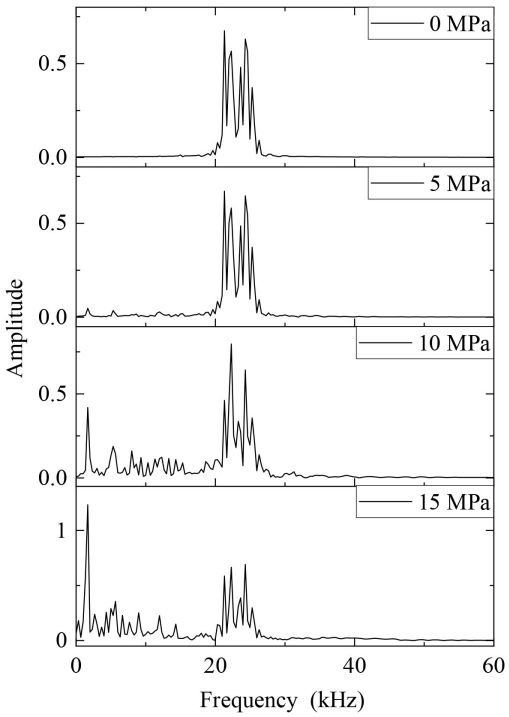

Figure 6. The change of frequency with confining pressure in absence of pull-out load.

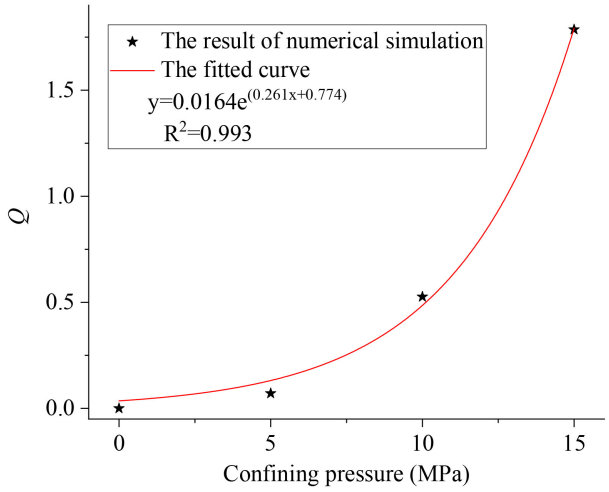

Figure 7. The relationship of Q and confining pressure without pull-out load.

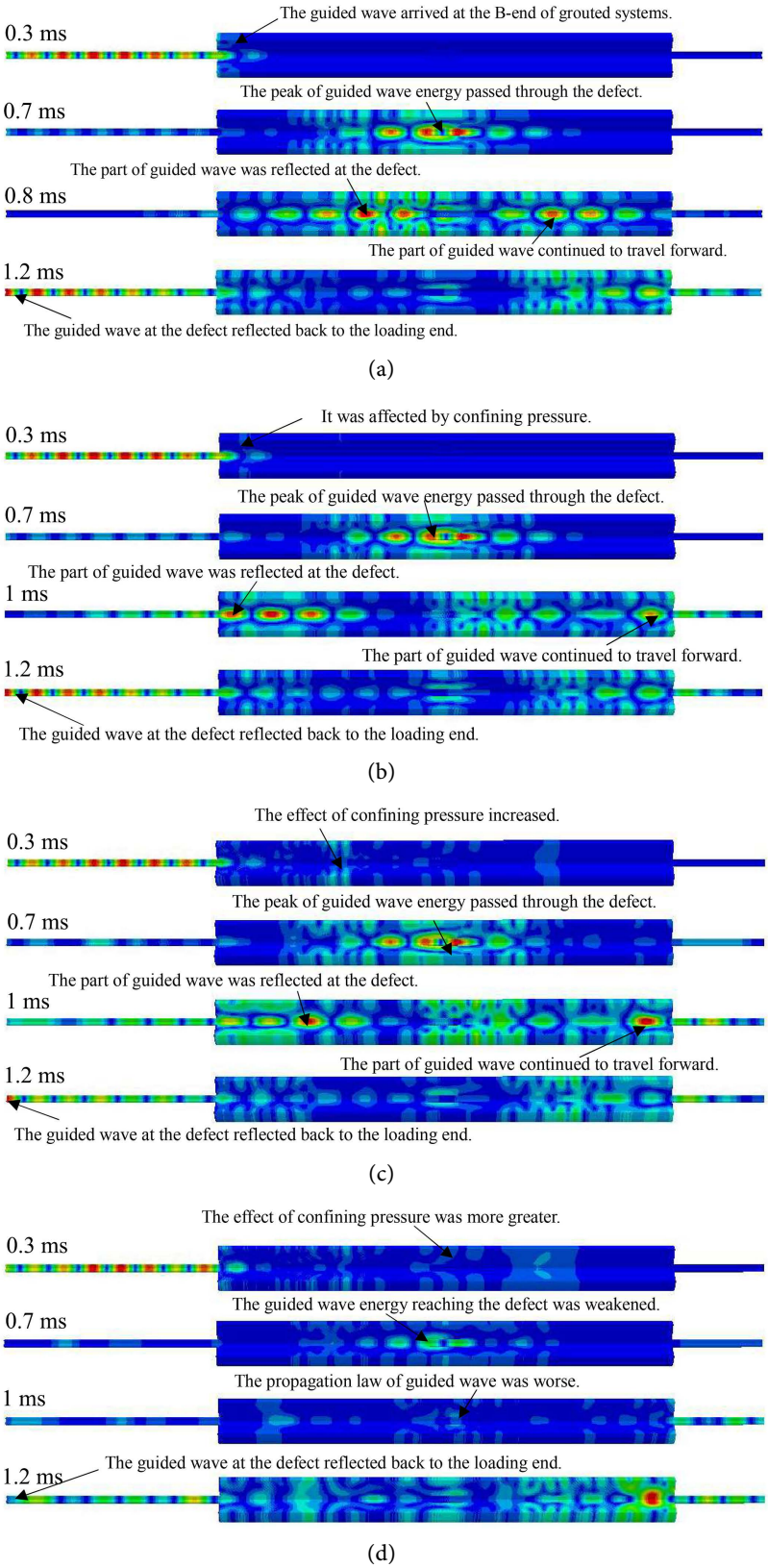

Figure 8. The guided wave propagation in grouted rockbolt systems under different confining pressure and in absence of pull-out load. (a) 0 MPa; (b) 5 MPa; (c) 10 MPa; (d) 15 MPa.

3.2. Effect of Confining Pressure on Guided Wave Propagation under Pull-Out Load

3.2.1. Under the Same Pull-Out Load and Different Confining Pressures

When the pull-out load is 50 kN, the propagation law of the guided wave under different confining pressures is shown in Figure 9. Under the same pull-out load, when the confining pressure is 0 MPa, the concrete is less restrictive, the rockbolt has a longer debonding length, and the guided wave propagation is more disordered due to the increased interference. With increasing confining pressure, the radial force of rockbolt systems increases, and the adhesion between the rockbolt and cement mortar increases, which leads to the restriction of the rockbolt, so the debonding length of the rockbolt gradually decreases, the bond quality increases, the law of guided wave propagation increases, and the echoes at the bond defects are gradually visible. Therefore, the confining pressure has a strengthening effect on the guided wave propagation law compared with the pull-out load, and the larger the confining pressure is, the stronger the strengthening effect is under the same pull-out load.

Under the action of a 50 kN pull-out load, the change in frequency in the guided wave with the confining pressure is shown in Figure 10. With the increase in the confining pressure, the low frequency part of the guided wave frequency in the rockbolt decreases, while the high frequency part increases, and the Q value (Figure 11) decreases exponentially with the increase in the confining pressure. This indicates that the confining pressure plays a strengthening role in the law of guided wave propagation under the same pull-out load.

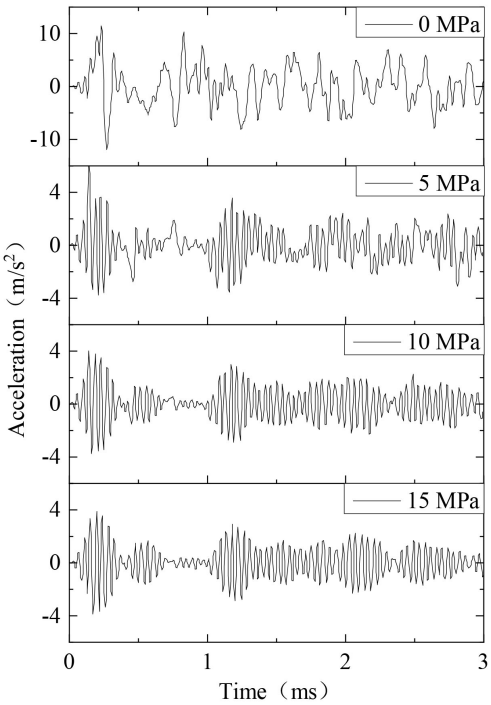

Figure 9. The influence of confining pressure on guided wave propagation law under 50 kN pull-out load.

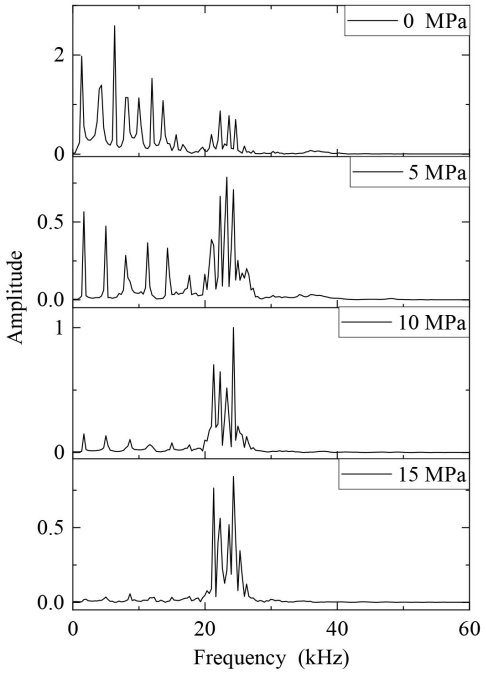

Figure 10. The change of frequency with the confining pressure under 50 kN pull-out load.

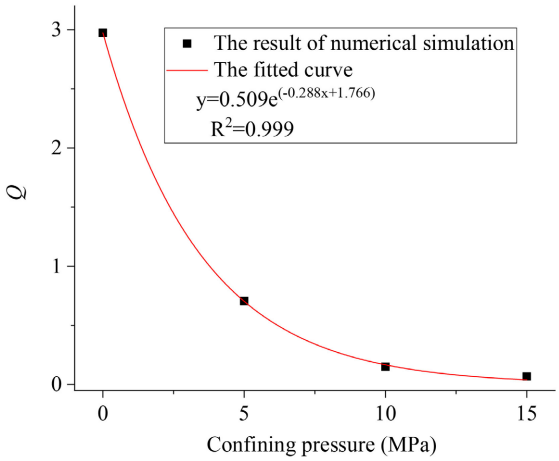

Figure 11. The relationship of Q and confining pressure under pull-out load.

Figure 12 displays a three-quarter model of the cylinder sample (The two-dimensional axisymmetric model was rotated around the symmetry axis to obtain the three-dimensional model in Abaqus) and shows the propagation process of the guided wave under different confining pressures when the pull-out load is 50 kN. When there is no confining pressure, the propagation process of the guided wave under the pull-out load of 50 kN is not very regular, but with the increase in the confining pressure, it can be clearly seen gradually that the peak energy of the guided wave reaches the bond defect, and the reflected wave occurs at the bond defect. At 1.2 ms, the return wave at the bond defect reaches the loading end, and the law of the guided wave propagation is enhanced. The guided

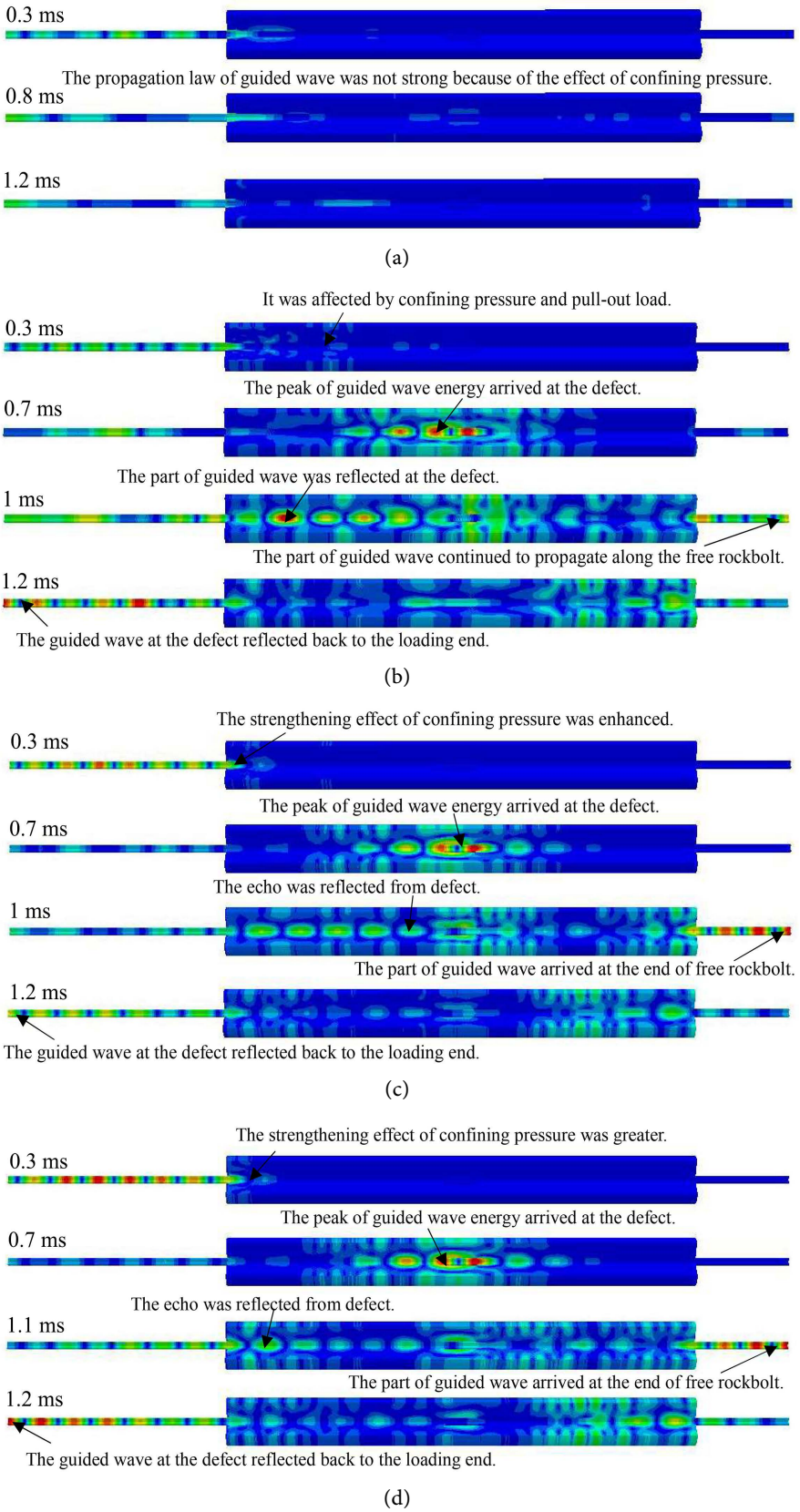

Figure 12. The influence of confining pressure on guided wave propagation process under 50 kN pull-out load. (a) 0 MPa; (b) 5 MPa; (c) 10 MPa; (d) 15 MPa.

wave propagation cloud map further reflects the strengthening effect of the confining pressure on the guided wave propagation law under the pull-out load under the same confining pressure and different pull-out loads.

3.2.2. Under the Same Confining Pressure and Different Pull-Out Loads

When the confining pressure is 10 MPa, the propagation law of the guided wave under different pull-out loads is shown in Figure 13. Without a pull-out load, the propagation law of the guided wave is affected by the confining pressure, and the wave packet oscillates slightly. The confining pressure weakens the guided wave propagation, but the echo at the bond defect is still clearly visible. However, when the pull-out load increases to 50 kN and 75 kN, the law of guided wave propagation gradually weakens, and the bond quality of the rockbolt also worsens, especially under the 75 kN pull-out load, and the echo at the bond defect can hardly be seen. The above phenomenon reflects that the pull-out load under the same confining pressure has a weakening effect on the guided wave propagation law, and the larger the pull-out load is, the more obvious the weakening effect is, resulting in the less obvious bond defect echo received at the A-end.

Figure 14 shows the variation in the frequency of the guided wave with the drawing load under a confining pressure of 10 MPa. When there is no pull-out load, the confining pressure weakens the law of guided wave propagation, and the Q value is relatively large. When the pull-out load increases to 50 kN, the high-frequency part of the guided wave increases, and the low-frequency part decreases. This is mainly due to the combined effect of the confining pressure and the pull-out load, and the strengthening effect of the confining pressure is

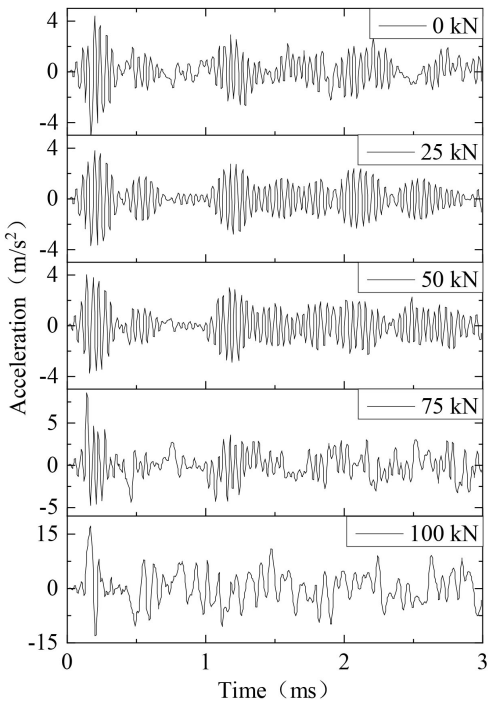

Figure 13. The influence of pull-out load on guided wave propagation law under 10 MPa confining pressure.

stronger than the weakening effect of the pull-out load, which dominates, leading to the reduction in the Q value (see Figure 15). When the pull-out load increases to 75 kN and 100 kN, the high frequency part decreases, the low frequency part increases, and the frequency in the guided wave shifts to the low frequency. It can be seen in Figure 15 that the Q value decreases first and then increases with increasing pull-out load in a quadratic polynomial function relationship, and the rockbolt anchoring bond quality decreases.

Figure 16 displays the propagation process of the guided wave under different pull-out loads under the action of a 10 MPa confining pressure. At first, the guided wave is only affected by the confining pressure. In the cloud chart, the guided wave propagation process is relatively good. At 0.7 ms, the peak of the

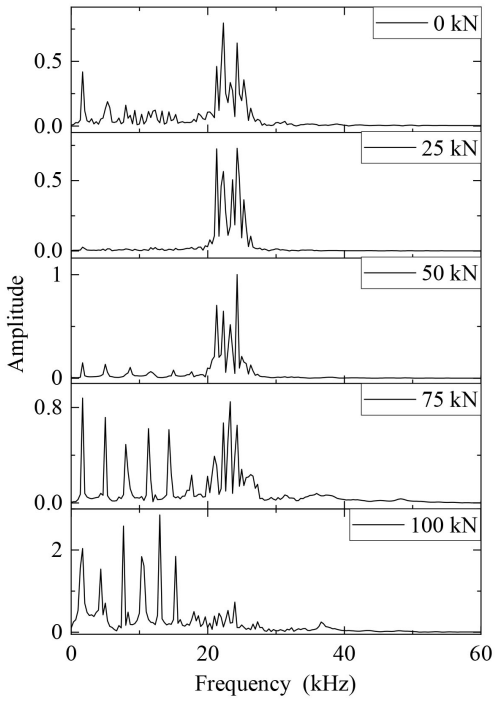

Figure 14. The change of frequency with pull-out load under 10 MPa confining pressure.

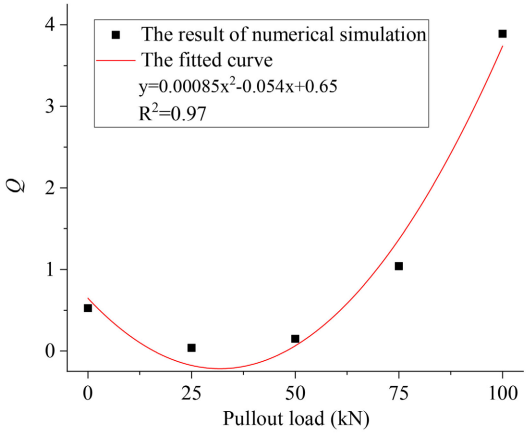

Figure 15. The relationship of Q and pull-out load under 10 MPa confining pressure.

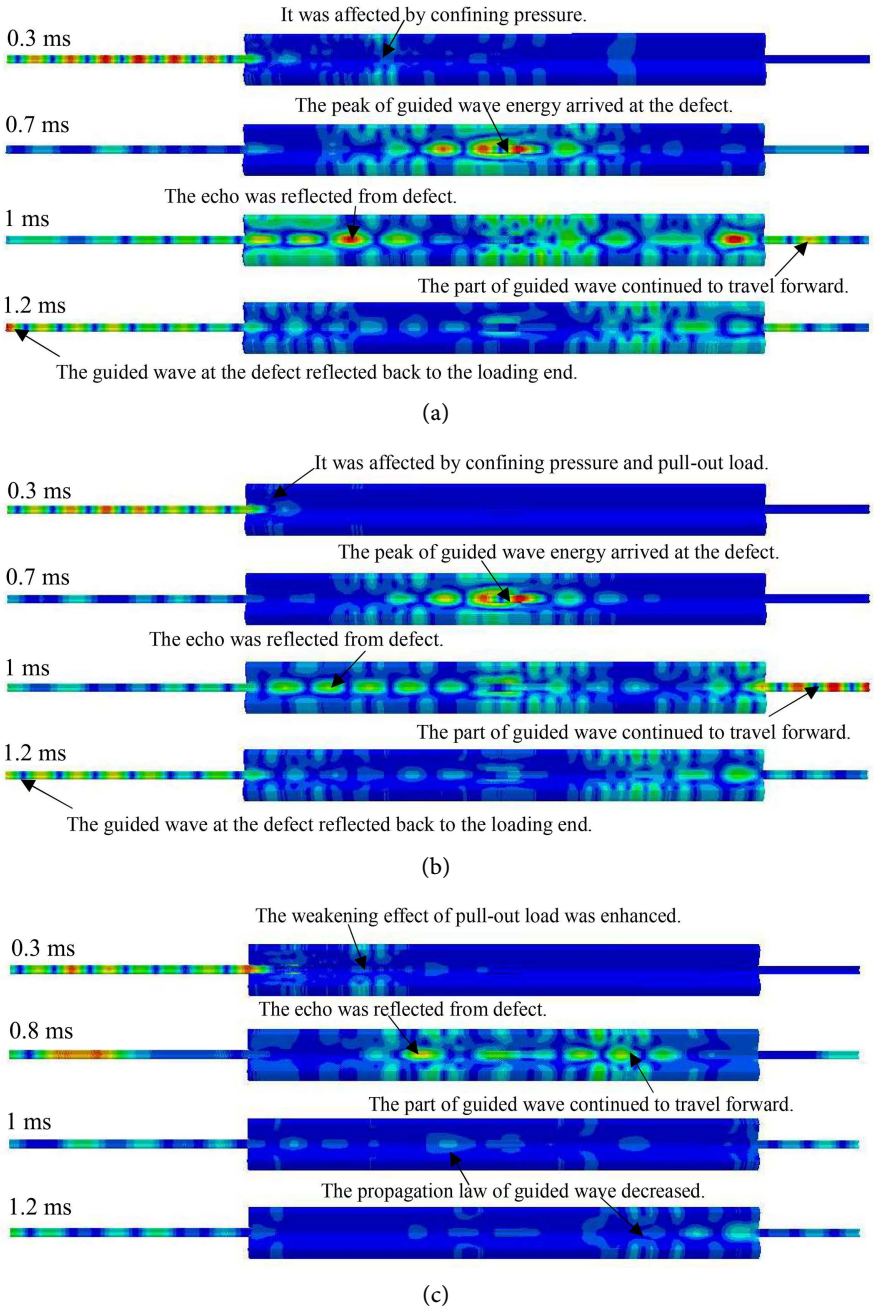

Figure 16. The influence of pull-out load on guided wave propagation process under 10 MPa confining pressure. (a) 0 kN; (b) 50 kN; (c) 75 kN.

guided wave energy reaches the bond defect, and then part of the energy is reflected back to the loading end of the anchorage systems at the bond defect, while part of the energy continues to propagate to the far end of the anchorage systems. However, under the action of 50 kN and 75 kN pull-out loads, some rockbolts debonded, and the adhesion between the rockbolts and cement mortar weakened. At the same time, under the action of confining pressure, the friction resistance between the rockbolts and cement mortar increases at the debonding point of the rockbolts, resulting in increased energy dissipation of the guided

wave in the process of propagation, and the law of guided wave propagation weakens. Therefore, under the same confining pressure, with the increase in the pull-out load, the rock bond quality of the rock rod will gradually deteriorate.

4. Conclusions

In this study, the propagation law of guided waves in grouted rockbolt systems with bond defects under the combined action of confining pressure and pull-out load is studied by numerical simulation, the propagation law of guided waves under the combined action of different pull-out loads and confining pressure is analysed, the bond quality of the rockbolt is determined, and the following conclusions are obtained:

1) In the absence of a pull-out load, with increasing confining pressure, the guided wave propagation law gradually worsens, and the echo wave packet at the bond defect also fluctuates with increasing confining pressure. The existence of a bond defect cannot change the weakening effect of the confining pressure on the guided wave propagation law.

2) Under the same pull-out load, with increasing confining pressure, the radial stress of the grouted rockbolt systems increases, and the bond between the rockbolt and cement mortar increases, resulting in reinforcement of the restraint of the rockbolt, and the law of guided wave propagation also increases gradually. The confining pressure plays a strengthening role in guided wave propagation.

3) Under the same confining pressure, with increasing pull-out load, part of the rockbolt debonding occurs, and the adhesion between the rockbolt and cement mortar weakens. However, at the debonding point of the rockbolt, the confining pressure increases the friction resistance between the rockbolt and the cement mortar, resulting in an increase in the energy dissipation of the guided wave in the propagation process and the weakening effect of the propagation law of the guided wave.

Acknowledgements

This work is funded by the National Science Foundation of China (Grant No. 52104157). This support is gratefully acknowledged.

Data Availability

The data used to support the findings of this study are included within the article.

Conflicts of Interest

The authors declare no conflicts of interest.

References

[1] He, M.C., Xie, H.P., Peng, S.P. and Jiang, Y.D. (2005) *Chinese of Journal Rock Mechanics and Engineering*, **24**, 2803-2813.

[2] Xu, F., Wang, K., Wang, S.G., Li, W.W., Liu, W.Q. and Du, D.S. (2018) *Construction and Building Materials*, **185**, 264-274. https://doi.org/10.1016/j.conbuildmat.2018.07.050

[3] Xu, C., Li, Z.H., Wang, S.Y., Wang, S.R., Tang, C.A., *et al.* (2018) *Rock Mechanics and Rock Engineering*, **51**, 861-871. https://doi.org/10.1007/s00603-017-1373-1

[4] Lin, Y.F., Ye, J.W. and Lo, C.M. (2022) *Construction and Building Materials*, **316**, Article ID: 125904. https://doi.org/10.1016/j.conbuildmat.2021.125904

[5] Cui, Y. and Zou, D.H. (2012) *Journal of Applied Geophysics*, **79**, 64-70. https://doi.org/10.1016/j.jappgeo.2011.12.010

[6] Srivastava, L.P. and Singh, M. (2015) *Engineering Geology*, **197**, 103-111. https://doi.org/10.1016/j.enggeo.2015.08.004

[7] Ghadimi, M., Shahriar, K. and Jalalifar, H. (2015) *Tunnelling and Undergroud Space Technology*, **50**, 143-151. https://doi.org/10.1016/j.tust.2015.07.014

[8] Nie, W., Zhao, Z.Y., Ma, S.Q. and Guo, W. (2018) *Tunnelling and Underground Space Technology*, **71**, 15-26. https://doi.org/10.1016/j.tust.2017.07.005

[9] Cui, Y. and Zou, D.H. (2006) *Journal of Applied Geophysics*, **59**, 337-344. https://doi.org/10.1016/j.jappgeo.2006.04.003

[10] Zhang, J.K., Li, K., Zhang, H., Wang, N., Guo, Q.L. and Zhao, L.Y. (2021) *Chinese of Journal Rock Mechanics and Engineering*, **40**, 1460-1472. http://rockmech.whrsm.ac.cn/EN/10.13722/j.cnki.jrme.2020.0630

[11] Zhang, L., Huang, Z.M., Bai, L., Ma, Z.G., Mao, X.B. and Chen, Z.Q. (2021) *Journal of China University Mining Technology*, **50**, 1077-1086.

[12] Wang, Y.K. Mukherjee, A. and Castel, A. (2022) *Construction and Building Materials*, **360**, Article ID: 129346. https://doi.org/10.1016/j.conbuildmat.2022.129346

[13] Liu, L.L., Zhu, J., Zhang, S.H. and Sun, P.H. (2022) *Earth Sciences*.

[14] Liu, X.C., Wu, B., Qin, F., He, C.F. and Han, Q. (2017) *Ultrasonics*, **73**, 196-205. https://doi.org/10.1016/j.ultras.2016.08.014

[15] Yu, S.S., Zhu, W.C. and Niu, L.L. (2022) *International Journal of Coal Science and Technology*, **9**, 8-15. https://doi.org/10.1007/s40789-022-00482-4

[16] Ivanovic, A. and Neilson, R.D. (2013) *International Journal of Rock Mechanics and Mining Science*, **64**, 36-43. https://doi.org/10.1016/j.ijrmms.2013.08.017

[17] Yu, S.S., Niu, L.L., Chen, J., Wang, Y.W. and Yang, H.H. (2022) *Advances in Materials Science and Engineering*, **2022**, Article ID: 3282211. https://doi.org/10.1155/2022/3282211

[18] Yu, S.S., Niu, L.L. and Chen, J. (2022) *Shock and Vibration*, **2022**, Article ID: 7012510. https://doi.org/10.1155/2022/7012510

[19] Yu, S.S., Zhu, W.C., Niu, L.L., Zhou, S.C. and Kang, P.H. (2021) *Tunnelling and Underground Space Technology*, **85**, 56-66. https://doi.org/10.1016/j.tust.2018.12.001

[20] Lee, J. and Fenves, G.L. (1998) *Journal of Engineering Mechanics*, **124**, 892-900. https://doi.org/10.1061/(ASCE)0733-9399(1998)124:8(892)

[21] Dassault Systemses Simulia (2014) ABAQUS Theory Manual & Users Manuals Version 6.11.

[22] Henriques, J., Silva, L.S. and Valente, I.B. (2013) *Engineering Structures*, **52**, 747-761. https://doi.org/10.1016/j.engstruct.2013.03.041

[23] Park, K., Ha, K., Choi, H. and Lee, C. (2015) *Cement and Concrete Composites*, **63**, 122-131. https://doi.org/10.1016/j.cemconcomp.2015.07.008

[24] Chang, C., Wang, G.Z., Liang, Z.Z., Yang, J.H. and Tang, C.A. (2017) *Construction and Building Materials*, **135**, 665-673. https://doi.org/10.1016/j.conbuildmat.2017.01.031

[25] Henriques, J., Gentili, F., Simoes da Silva, L. and Simoes, R. (2015) *Engineering Structures*, **87**, 86-104. https://doi.org/10.1016/j.engstruct.2014.12.039

[26] Yang, W.R., He, X.J. and Dai, L. (2017) *Composite Structures*, **161**, 173-186. https://doi.org/10.1016/j.compstruct.2016.11.041

[27] Rezazadeh, M., Carvelli, V. and Veljkovic, A. (2017) *Construction and Building Materials*, **153**, 102-116. https://doi.org/10.1016/j.conbuildmat.2017.07.092

[28] Martin, L.B., Tijani, M., Hassen, F.H. and Noiret, A. (2013) *International Journal of Rock Mechanics and Mining Science*, **63**, 50-61. https://doi.org/10.1016/j.ijrmms.2013.06.007